

Improving self-supervised pretraining models for epileptic seizure detection from EEG data

Sudip Das¹, Pankaj Pandey¹, and Krishna Prasad Miyapuram¹

Computer Science and Engineering, IIT Gandhinagar, India

Abstract. There is abundant medical data on the internet, most of which are unlabeled. Traditional supervised learning algorithms are often limited by the amount of labeled data, especially in the medical domain, where labeling is costly in terms of human processing and specialized experts needed to label them. They are also prone to human error and biased as a select few expert annotators label them. These issues are mitigated by Self-supervision, where we generate pseudo-labels from unlabelled data by seeing the data itself. This paper presents various self-supervision strategies to enhance the performance of a time-series based Diffusion convolution recurrent neural network (DCRNN) model. The learned weights in the self-supervision pretraining phase can be transferred to the supervised training phase to boost the model’s prediction capability. Our techniques are tested on an extension of a Diffusion Convolutional Recurrent Neural network (DCRNN) model, an RNN with graph diffusion convolutions, which models the spatiotemporal dependencies present in EEG signals. When the learned weights from the pretraining stage are transferred to a DCRNN model to determine whether an EEG time window has a characteristic seizure signal associated with it, our method yields an AUROC score 1.56% than the current state-of-the-art models on the TUH EEG seizure corpus.

Keywords: Pretraining · self-supervision · supervised models · Epileptic seizure · Electroencephalogram · DCRNN.

1 Introduction

A seizure is the occurrence of an abnormal, intense discharge of a batch of cortical neurons. Epilepsy is a condition of the central nervous system characterized by repeated seizures. The distinction between epilepsy and seizure is important because of the fact their treatments are different [24]. For epilepsy diagnosis, at least two unprovoked seizures should happen in quick succession. The risk of premature death in people with epilepsy is about three times that of the general population [1]. The EEG or electroencephalogram is an electrophysiological-based technique for measuring the electrical activity emerging from the human brain normally recorded at the brain scalp.

It is widely accepted that EEG originates from cortical pyramidal neurons [7] that are positioned perpendicular to the brain’s surface. The EEG records

the neural activity, which is the superimposition of inhibitory and excitatory postsynaptic potentials of a sizeable group of neurons discharging synchronously. Cortical neurons are the electrically excitable cells present in the central nervous system. Through a special type of connection known as synapses, the information is communicated and processed in these neurons by electrochemical signaling.

Scalp Electroencephalogram (EEG) is one of the main diagnostic tests in neurology for detecting epileptic seizures. Most patients demonstrate some characteristic aberrations during an epileptic seizure [2]. A drawback in using EEG signals for clinical diagnosis is that the cerebral potential may change quite drastically by muscle movements or even the environment. The resultant EEG signal contains artifacts that make it harder to provide a diagnosis to the affected patients. Most of the medical data available publicly are unlabeled [21]. Many approaches like semi-supervised learning and self-supervised learning have used the unlabeled data for training.

2 Self-supervision in the medical domain

There is an abundance of medical data on the internet, most of them being unlabeled. Traditional machine learning (ML) algorithms use labeled data to train supervised models. These unlabeled data are of no use to supervised models.

Self-supervised learning (SSL) methods, as the name suggests, use some form of supervision. Using self-supervision, the labels are extracted from the data by using a fixed pretext task. The task makes use of the innate structure of the input data [15]. Some of the basic pretext tasks are given in figure 1. This strategy works well on images, as was proved in the ImageNet challenge [28]. Self-supervision models such as SimCLR [13] and BYOL [16] perform well in image classification tasks even if they use 1% of the ground truth labels. They give performance comparable to the fully self-supervision tasks. It also works well on time series data such as natural language [20], audio and speech understanding [8].

In the Works of [5,40,40], they tried to prove the usefulness of self-supervision and the qualities of a reliable self-supervision pretext task. In predictive learning, the representations of unlabeled data are learned by predicting masked time series data. Recent works [30] on time series data have shown how a contrastive learning technique can be reduced to a masking problem. However, most of these works are focused on computer vision or text-related applications, and very few of them use EEG data.

In this work, we use different self-supervised strategies where we use the unlabelled data to increase the performance of supervised models. These strategies help the model learn natural features from the dataset, which helps the model distinguish diseased Electroencephalogram (EEG) signals from the healthy ones.

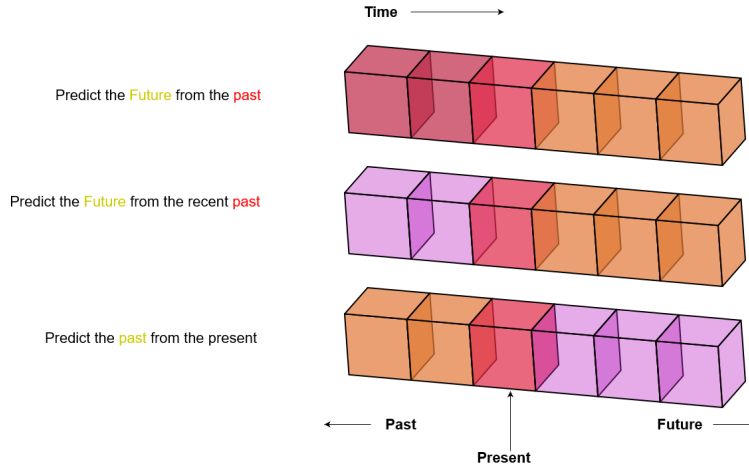


Fig. 1. Basic pretext tasks for time series data

3 Related works

There has been a shift from using convolutional neural networks (CNNs) to combining CNN and Graph neural networks. Many studies in this domain [4, 6, 26, 27], assume euclidean structures in EEG signals. The application of 3D-CNN on the EEG spectrogram of the signals violates the natural geometry of EEG electrodes and the connectivity in the brain signals. EEG electrodes are placed on a person’s scalp and hence are non-euclidean. The natural geometry of EEG electrodes is best represented on a graph [10, 12]. In [38], the authors use GNN to extract feature vectors and then use convolution on the intermediate results. Whereas in [37] they extract features using Power Spectral Density (PSD) which are used as the node vectors, and perform spectral graph convolutions [18]. Graph representation learning has been used heavily in modeling brain networks [11]. Recent models such as [34] outperforms previous CNN based methods [29] and CNN based Long short-term memory-based methods [4]. In [34], they use self-supervision to increase the performance of the supervision models. Specifically, they pre-train the model on the 12/60s of EEG clip for predicting the next T' second EEG clip and transfer the learning to the model’s encoder. Some studies [9, 19, 23, 41] used a different pretraining strategy but did not use any graph-based methods to model the EEG signals.

4 Experimental setup

4.1 Dataset

For our testing, we used the publicly available Temple university hospital EEG Seizure corpus (TUSZ) v1.5.2. [31], which is the largest publicly available seizure

corpus to date with 5,612 EDF files, 3,050 annotated seizures from clinical recordings, and eight seizure types. Five subjects were present both in the TUSZ train and test subjects, thus not considered in our self-supervision strategy. The validation split was created from the train split by randomly selecting 10% of the subjects from the train split. This was done to ensure the test and validation performance reflects the performance of unseen subjects as seen in real-world scenarios.

Since epileptic seizures have a specific frequency range in the EEG signal. [35], and hence it is intuitive to convert the raw EDF files into the frequency domain. The log amplitudes are obtained after applying the Fast Fourier transformation to all the non-overlapping 12s windows. This is done for all the windows for faster pre-processing.

	EEG files (% Seizure)	Patients (% Seizure)	Total Duration (Sec)	Seizure Duration (Sec)
Train files	4599 (18.9%)	4599 (34.1%)	2710483	169793 (6.6%)
Test files	900 (25.6%)	45 (77.8%)	541895	53105 (9.8%)

Table 1. Detailed summary of TUSZ v1.5.2

5 Graph neural network for EEG signals

5.1 Representing EEG’s as graphs

Multivariate time-series of EEG signals can be modeled as a graph G , where $G = V, E, W$. Here V denotes the electrodes/channels, E denotes the set of edges, and W is the adjacency matrix. Two types of graphs were formed according to [34] to validate our self-supervision strategies.

Distance Graph: To capture the natural geometry of the brain, edge weights are computed between two electrodes v_i and v_j is the distance between them, i.e.

$$W_{ij} = \exp\left(-\frac{\text{dist}(v_i, v_j)^2}{\sigma^2}\right) \quad \text{if } \text{dist}(v_i, v_j) \leq \kappa \quad (1)$$

Where κ is the threshold produced by a Gaussian kernel [32], which generates a sparse adjacency matrix, and σ is the standard deviation of the distances. This results in a weighted undirected graph for the EEG windows. The κ is set at 0.9 as it resembles the EEG montage widely used in the medical domain [3].

Correlation graph: The edge weight W_{ij} is computed as the absolute value of the cross-correlation between the electrode signals v_i and v_j , normalized across the graph. To keep the more influential edges and introduce sparsity, the top 3 neighbors for each node are kept, excluding self-edges.

5.2 DCRNN for EEG signals

A Diffusion Convolutional Recurrent neural network (DCRNN) [22] models the *spatiotemporal dependencies* in EEG signals. DCRNN was initially proposed for traffic forecasting on road networks, where it is modeled as a diffusion process. The objective is to learn a function that predicts the future traffic speeds of a sensor network given the historic traffic speeds.

The spatial dependency of the EEG signals is similar to the traffic forecasting problem and is modeled as a diffusion process on a directed graph. This is because an electrode has an influence over other electrodes given by the edge weights. DCRNN captures spatial and temporal dependencies among time series using diffusion convolution, sequence to sequence learning framework, and scheduled sampling.

Diffusion Convolution The diffusion process is characterized by a bidirectional random walk on a directed graph signal G . Whereas the diffusion convolution operation over a graph signal $X \in R^{N \times P}$ and a filter f_θ is defined as:

$$X_{:,p} \star_G f_\theta = \sum_{k=0}^{K-1} (\theta_{k,1}(D_O^{-1}W)^k + \theta_{k,2}(D_I^{-1}W^T)^k)X_{:,p} \quad \text{for } p \in \{1, \dots, P\} \quad (2)$$

where $X \in R^{N \times P}$ is the pre-processed EEG signal at a specific time instance $t \in \{1, \dots, T\}$ with N nodes and P features. Here $\theta \in R^{K \times 2}$ are the parameters of the filter and $D_O^{-1}W$, $D_I^{-1}W^T$ represent the transition matrices of the diffusion matrices of the inwards and outwards diffusion processes respectively [22].

For modeling the temporal dependency in EEG signals, Gated Recurrent units [14], a variant of Recurrent neural network (RNN) having a gating mechanism are used. To incorporate diffusion convolution, the matrix multiplications are replaced with diffusion convolutions [22]. For seizure detection, the model consists of several DCGRUs, stacked together and accompanied by a fully connected layer.

6 Self-Supervision Methods

We propose five pretraining strategies for time series data for model pretraining. These methods are tested on a $T = 12s$ window, having 19 channels and 200 time points. We denote the matrix corresponding to the EEG signal as $S \in R^{19 \times 200}$. The objective function is to predict the original signal given the noisy/masked signal. We use the mean absolute error between the predicted and the original EEG window as our loss function.

6.1 Jitter

The modified signal, S' was created by superimposing the main signal, S with a noise signal. The noise has the same mean, $\mu(S)$ and a fraction L of the

variance of the original signal. We set $L = 5\%$ as experimented by [17] for data augmentation. The random noise signal M from a normal distribution, is created as $M = N(\mu(S), 0.05 \cdot Var(S))$. Then,

$$S' = S + M \quad (3)$$

Since the magnitude of the noise is much lower compared to the EEG signal, the resultant signal had a small shift along the y-axis, as shown in Figure 2.

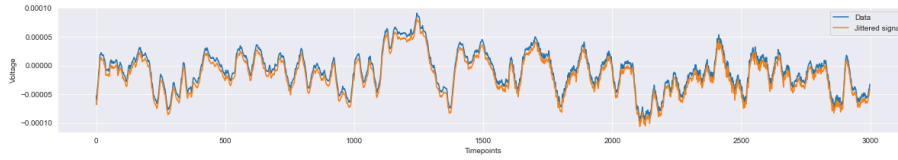


Fig. 2. EEG signal before and after introducing jitter

6.2 Random sample

The noisy signal is created by randomly choosing some fraction of the time points, i.e., t_1, t_2, \dots, t_k and replacing them with their neighbors' average [17]. For example, if neighbors of t_i are t_{i1}, t_{i2} then we replace t_i with $\frac{t_{i-1} + t_{i+1}}{2}$. The first and last points were not considered as they do not have both neighbors. We chose 20% of the points in each channel and replaced them with zeros, as shown in Figure 3. This has a "smoothing" effect on the initial graph as some data points which were local maxima/minima are now in the straight line connecting their neighbors.

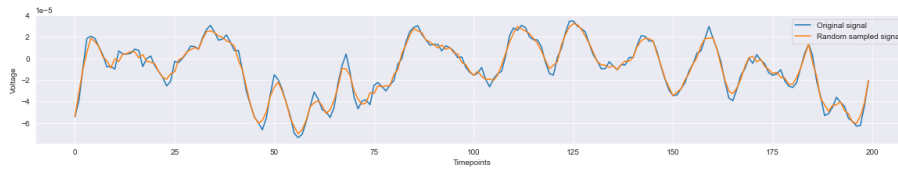


Fig. 3. EEG signal before and after introducing random sampling

6.3 Remove a specific channel

Trying to predict a channel by using the data from other channels clears the way for many different opportunities. It proves that a particular channel is a function of other channels and does not provide any new data.

We try to use this problem in our self-supervision. This can be done either by picking a random channel from each lobe or for all the channels. We select channel F3 from the Frontal lobe for this task. Mathematically, we set $S_{K,i} = 0$ for all i , where K is the channel number. For illustration purposes, Figure. 4 only uses the first five channels in which the channel F3 is replaced with zeros.

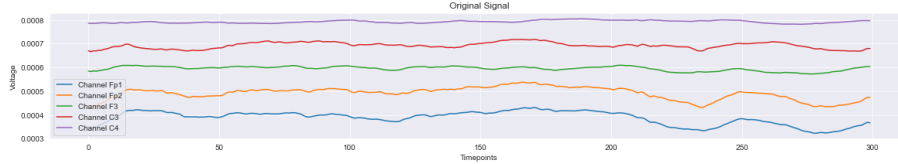


Fig. 4. Original signal with five channels

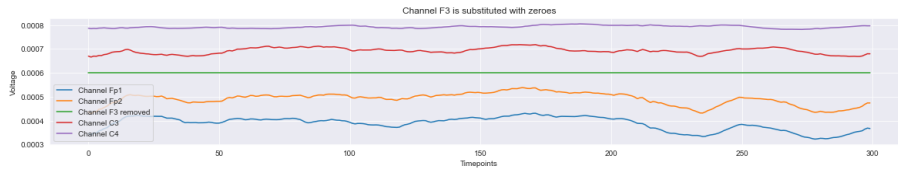


Fig. 5. Resultant signals after noise is added

6.4 Predicting windows

We select a small window from each channel instead of selecting all the points of a single channel. The noisy signal is created by replacing the selected time points with dummy points for all the channels.

In other words, we choose a window of length l randomly in each of the channels i and make entries from $j + 1$ to $j + l$ of that channel zero. So, for a particular channel i , $S_{i,j+1}, \dots, S_{i,j+l} = 0$. The window length l consists of 20% the total timepoints. These points are replaced with zeros. This is shown in Figure 6.

6.5 Jittering in random window

This method is a combination of methods 6.1 and 6.4. A noise having the same characteristics as in 6.1 is introduced in a small window having the same length as in 6.4. This method combines the advantages of both, as no essential data is being deleted but modified only in a selected window. In other words, we choose a window of length l randomly in each of the channels i . We generate a random

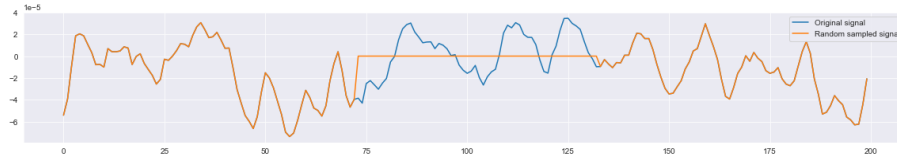


Fig. 6. Resultant signal after noise is added for a single channel

noise M with the same strategy as in 6.1, and introduce this noise in a window that is selected by 6.4. We use equation (3) for generating noise. Mathematically,

$$S'_{i,j+k} = S_{i,j+k} + 0.05 \cdot \text{Var}(M) \text{ for } k = 1 \text{ to } l. \quad (4)$$

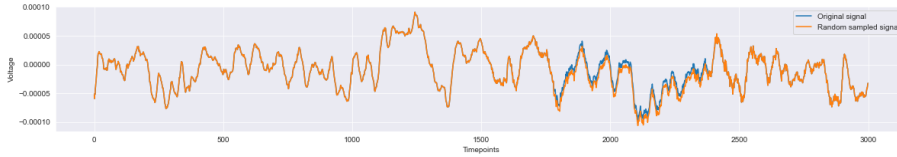


Fig. 7. A window is selected and noise is introduced

In Figure 7, a certain part of the signal has some modifications, while the rest is left unchanged.

7 Experimental results and analysis

7.1 Self-Supervision proposed techniques improves performance

Self-supervision is typically used when we want to use unlabeled data for training our model. In contrast, the TUSZ dataset used in our study is fully labeled. In works of [5, 40, 40] they tried to prove why self-supervision helps and what are the qualities of a reliable self-supervision pretext task. The study which we extended [34] also proves the same. We were able to improve the gap by using different pretraining strategies, especially on the distance-based graphs.

7.2 Model training

The AUROC score is the industry standard for evaluating models in the medical domain. It is prevalent for binary classification in medical domain [4, 6, 25]. Therefore, we use the AUROC score as the standard evaluation metric for evaluating our self-supervision strategies. The base model of predicting the next $T = 12s$, given the current $T = 12s$ in [34] has been replaced with these strategies. The

Table 2. Comparison of our proposed techniques with recent work

Seizure detection model	Seizure detection AUROC
Traditional algorithms [34]	
Dense-CNN	0.812 \pm 0.014
LSTM	0.786 \pm 0.014
CNN-LSTM	0.749 \pm 0.006
State of the art [34]	
Corr-DCRNN w/o Pre-training	0.812 \pm 0.012
Dist-DCRNN w/o Pre-training	0.824 \pm 0.020
Corr-DCRNN w/ Pre-training	0.861 \pm 0.005
Dist-DCRNN w/ Pre-training	0.866 \pm 0.016
Our SSL strategies	
Corr-Jittering w/Pre-training	0.8709 \pm 0.0047
Corr-Jittering in a random window w/pretraining	0.8658 \pm 0.0271
Corr-Remove channel (F3) w/Pre-training	0.8655 \pm 0.0035
Corr-Predicting windows w/Pre-training	0.8691 \pm 0.0040
Corr-Random sample w/Pre-training	0.8692 \pm 0.0042
Dist-Jittering w/Pre-training	0.8749 \pm 0.000053
Dist-Jittering in a random window	0.8759 \pm 0.000045
Dist-Remove channel (F3) w/Pre-training	0.8774 \pm 0.000035
Dist-Predicting windows w/Pre-training	0.8802 \pm 0.000012
Dist-Random sample w/Pre-training	0.8816 \pm 0.000006

batch size has been set to 1500, while the other hyperparameters have been set at the default values provided by [34]. Our pretraining and training were performed on a single NVIDIA RTX 5000 GPU. The self-supervision model parameters were randomly initialized for the pretraining phase. The DCGRU decoder model parameters were randomly initialized, and the encoder weights were set to the same weights as that of the self-supervision encoder.

7.3 Outperform the state-of-the-art

We compare our five self-supervision models with the previous state-of-the-art in Table 2. For each strategy and type of graph, we ran the pretraining twice. We took five training runs for each self-supervision strategy to get a reliable estimate. The mean and standard deviation are computed across all the models.

The self-supervision model weights are transferred to the encoder of the seizure classification model for each run and then trained on the labeled windows. With these changes applied, we were able to surpass the state-of-the-art results by 1.56% after applying this simple modification.

7.4 Low deviation during Dist-Graph Compared to Correlation Graph

The correlation-based graphs either produced very marginal improvement or had a lower score compared to the state-of-the-art. We set the number of epochs for pretraining and training as 350 and 100, respectively. The loss function for the distance-based graph converged in both the training and testing phases over all the epochs. In contrast, the loss function for correlation-based graphs converged faster at a higher value than their distance-based counterparts. The correlation-based models were stopped early since we did not see any improvements. This happened during both the training and testing phases. This resulted in a higher standard deviation and a lower AUROC score than their respective distance-based counterparts.

We noted that in papers [33, 34, 36, 39], they used spatial connectivity as well as distance functional connectivity. For spatial connectivity, they used a distance-based graph, either the Euclidean distance or the actual measured between two points of a sphere. For functional connectivity, they have used a binary relationship between the electrodes. The purpose of using functional connectivity is to exploit the dynamic nature of time-series data. To validate our results, we randomly re-ran two of these five strategies for both types of graphs, and our results were within the margin of error.

8 Conclusion and future work

A notable point in our results is the difference in the magnitude of the standard deviation. The order of magnitude of the correlation-based models is similar to that of the previous state-of-the-art models. However, it is considerably more precise in distance-based models. The distance graphs consistently outperformed the correlation-based graphs and benefitted the most after using these five SSL strategies. The distance-based random sampling model performed the best among all the models, whereas the correlation-based random sampling model came in a close second among the correlation-based ones. We outperformed the previous state-of-the-art by introducing the self-supervision strategy, and the training phase was kept as it is. Our future work will focus on testing our proposed novel self-supervision strategies to other time-series data.

Acknowledgement

We thank Science and Engineering Research Board (SERB) and PlayPower Labs for supporting the Prime Minister’s Research Fellowship (PMRF) awarded to Pankaj Pandey. We thank Federation of Indian Chambers of Commerce & Industry (FICCI) for facilitating this PMRF.

References

1. Epilepsy, <https://www.who.int/news-room/fact-sheets/detail/epilepsy>
2. Electroencephalography (eeg): An introductory text and atlas of normal and abnormal findings in adults, children, and infants [internet]. Chicago: American Epilepsy Society (2016)
3. Acharya, J.N., Hani, A.J., Cheek, J., Thirumala, P., Tsuchida, T.N.: American clinical neurophysiology society guideline 2: guidelines for standard electrode position nomenclature. *The Neurodiagnostic Journal* **56**(4), 245–252 (2016)
4. Ahmedt-Aristizabal, D., Fernando, T., Denman, S., Robinson, J.E., Sridharan, S., Johnston, P.J., Laurens, K.R., Fookes, C.: Identification of children at risk of schizophrenia via deep learning and eeg responses. *IEEE journal of biomedical and health informatics* **25**(1), 69–76 (2020)
5. Arora, S., Khandeparkar, H., Khodak, M., Plevrakis, O., Saunshi, N.: A theoretical analysis of contrastive unsupervised representation learning. arXiv preprint arXiv:1902.09229 (2019)
6. Asif, U., Roy, S., Tang, J., Harrer, S.: SeizureNet: Multi-spectral deep feature learning for seizure type classification. In: *Machine Learning in Clinical Neuroimaging and Radiogenomics in Neuro-oncology*, pp. 77–87. Springer (2020)
7. Avitan, L., Teicher, M., Abeles, M.: Eeg generator—a model of potentials in a volume conductor. *Journal of neurophysiology* **102**(5), 3046–3059 (2009)
8. Bai, J., Wang, W., Zhou, Y., Xiong, C.: Representation learning for sequence data with deep autoencoding predictive components. arXiv preprint arXiv:2010.03135 (2020)
9. Banville, H., Chehab, O., Hyvärinen, A., Engemann, D.A., Gramfort, A.: Uncovering the structure of clinical eeg signals with self-supervised learning. *Journal of Neural Engineering* **18**(4), 046020 (2021)
10. Bronstein, M.M., Bruna, J., LeCun, Y., Szlam, A., Vandergheynst, P.: Geometric deep learning: going beyond euclidean data. *IEEE Signal Processing Magazine* **34**(4), 18–42 (2017)
11. Bullmore, E., Sporns, O.: Complex brain networks: graph theoretical analysis of structural and functional systems. *Nature reviews neuroscience* **10**(3), 186–198 (2009)
12. Chami, I., Abu-El-Haija, S., Perozzi, B., Ré, C., Murphy, K.: Machine learning on graphs: A model and comprehensive taxonomy. arXiv preprint arXiv:2005.03675 (2020)
13. Chen, T., Kornblith, S., Norouzi, M., Hinton, G.: A simple framework for contrastive learning of visual representations. In: *International conference on machine learning*, pp. 1597–1607. PMLR (2020)
14. Cho, K., van Merriënboer, B., Bahdanau, D., Bengio, Y.: On the properties of neural machine translation: Encoder–decoder approaches. In: *Proceedings of SSTS-8, Eighth Workshop on Syntax, Semantics and Structure in Statistical Translation*, pp. 103–111. Association for Computational Linguistics, Doha, Qatar (Oct 2014). <https://doi.org/10.3115/v1/W14-4012>, <https://aclanthology.org/W14-4012>
15. Doersch, C., Gupta, A., Efros, A.A.: Unsupervised visual representation learning by context prediction. In: *Proceedings of the IEEE international conference on computer vision*, pp. 1422–1430 (2015)
16. Grill, J.B., Strub, F., Altché, F., Tallec, C., Richemond, P., Buchatskaya, E., Doersch, C., Avila Pires, B., Guo, Z., Gheshlaghi Azar, M., et al.: Bootstrap your own latent—a new approach to self-supervised learning. *Advances in Neural Information Processing Systems* **33**, 21271–21284 (2020)

17. Jayarathne, I., Cohen, M., Amarakeerthi, S.: Person identification from eeg using various machine learning techniques with inter-hemispheric amplitude ratio. *PloS one* **15**(9), e0238872 (2020)
18. Kipf, T.N., Welling, M.: Semi-supervised classification with graph convolutional networks. arXiv preprint arXiv:1609.02907 (2016)
19. Kostas, D., Aroca-Ouellette, S., Rudzicz, F.: Bendr: using transformers and a contrastive self-supervised learning task to learn from massive amounts of eeg data. *Frontiers in Human Neuroscience* **15** (2021)
20. Lan, Z., Chen, M., Goodman, S., Gimpel, K., Sharma, P., Soricut, R.: Albert: A lite bert for self-supervised learning of language representations. arXiv preprint arXiv:1909.11942 (2019)
21. LeCun, Y.: I'm giving the introductory keynote at the international solid state circuit conference in san francisco this morning at 8:45 pst.slides here: <https://t.co/uqyx4hphyl> (Feb 2019), <https://twitter.com/ylecun/status/1097532314614034433>
22. Li, Y., Yu, R., Shahabi, C., Liu, Y.: Diffusion convolutional recurrent neural network: Data-driven traffic forecasting. arXiv preprint arXiv:1707.01926 (2017)
23. Martini, M.L., Valliani, A.A., Sun, C., Costa, A.B., Zhao, S., Panov, F., Ghatan, S., Rajan, K., Oermann, E.K.: Deep anomaly detection of seizures with paired stereoelectroencephalography and video recordings. *Scientific Reports* **11**(1), 1–11 (2021)
24. An introduction to epilepsy. Chicago: American Epilepsy Society (2006)
25. O'Shea, A., Lightbody, G., Boylan, G., Temko, A.: Neonatal seizure detection from raw multi-channel eeg using a fully convolutional architecture. *Neural Networks* **123**, 12–25 (2020)
26. Raghu, S., Sriraam, N., Temel, Y., Rao, S.V., Kubben, P.L.: Eeg based multi-class seizure type classification using convolutional neural network and transfer learning. *Neural Networks* **124**, 202–212 (2020)
27. Rasheed, K., Qayyum, A., Qadir, J., Sivathamboo, S., Kwan, P., Kuhlmann, L., O'Brien, T., Razi, A.: Machine learning for predicting epileptic seizures using eeg signals: A review. *IEEE Reviews in Biomedical Engineering* **14**, 139–155 (2020)
28. Russakovsky, O., Deng, J., Su, H., Krause, J., Satheesh, S., Ma, S., Huang, Z., Karpathy, A., Khosla, A., Bernstein, M., et al.: Imagenet large scale visual recognition challenge. *International journal of computer vision* **115**(3), 211–252 (2015)
29. Saab, K., Dunnmon, J., Ré, C., Rubin, D., Lee-Messer, C.: Weak supervision as an efficient approach for automated seizure detection in electroencephalography. *NPJ digital medicine* **3**(1), 1–12 (2020)
30. Saunshi, N., Malladi, S., Arora, S.: A mathematical exploration of why language models help solve downstream tasks. arXiv preprint arXiv:2010.03648 (2020)
31. Shah, V., Von Weltin, E., Lopez, S., McHugh, J.R., Veloso, L., Golmohammadi, M., Obeid, I., Picone, J.: The temple university hospital seizure detection corpus. *Frontiers in neuroinformatics* **12**, 83 (2018)
32. Shuman, D.I., Narang, S.K., Frossard, P., Ortega, A., Vandergheynst, P.: The emerging field of signal processing on graphs: Extending high-dimensional data analysis to networks and other irregular domains. *IEEE signal processing magazine* **30**(3), 83–98 (2013)
33. Song, T., Zheng, W., Song, P., Cui, Z.: Eeg emotion recognition using dynamical graph convolutional neural networks. *IEEE Transactions on Affective Computing* **11**(3), 532–541 (2018)

34. Tang, S., Dunnmon, J., Saab, K.K., Zhang, X., Huang, Q., Dubost, F., Rubin, D., Lee-Messer, C.: Self-supervised graph neural networks for improved electroencephalographic seizure analysis. In: International Conference on Learning Representations (2021)
35. Tzallas, A.T., Tsipouras, M.G., Fotiadis, D.I.: Epileptic seizure detection in eegs using time–frequency analysis. *IEEE transactions on information technology in biomedicine* **13**(5), 703–710 (2009)
36. Varatharajah, Y., Chong, M.J., Saboo, K., Berry, B., Brinkmann, B., Worrell, G., Iyer, R.: Eeg-graph: a factor-graph-based model for capturing spatial, temporal, and observational relationships in electroencephalograms. *Advances in neural information processing systems* **30** (2017)
37. Wagh, N., Varatharajah, Y.: Eeg-gcnn: Augmenting electroencephalogram-based neurological disease diagnosis using a domain-guided graph convolutional neural network. In: *Machine Learning for Health*. pp. 367–378. PMLR (2020)
38. Wang, J., Liang, S., He, D., Wang, Y., Wu, Y., Zhang, Y.: A sequential graph convolutional network with frequency-domain complex network of eeg signals for epilepsy detection. In: *2020 IEEE International Conference on Bioinformatics and Biomedicine (BIBM)*. pp. 785–792. IEEE (2020)
39. Wang, X.h., Zhang, T., Xu, X.m., Chen, L., Xing, X.f., Chen, C.P.: Eeg emotion recognition using dynamical graph convolutional neural networks and broad learning system. In: *2018 IEEE International Conference on Bioinformatics and Biomedicine (BIBM)*. pp. 1240–1244. IEEE (2018)
40. Wei, C., Shen, K., Chen, Y., Ma, T.: Theoretical analysis of self-training with deep networks on unlabeled data. *arXiv preprint arXiv:2010.03622* (2020)
41. Xu, J., Zheng, Y., Mao, Y., Wang, R., Zheng, W.S.: Anomaly detection on electroencephalography with self-supervised learning. In: *2020 IEEE International Conference on Bioinformatics and Biomedicine (BIBM)*. pp. 363–368. IEEE (2020)